Nigerian Journal of Technology (NIJOTECH)
Vol. 39, No. 3, July 2020, pp. **767 – 775**

Print ISSN: 0331-8443, Electronic ISSN: 2467-8821
www.nijotech.com
http://dx.doi.org/10.4314/njt.v39i3.16

EFFECT OF DIFFERENT SYNGAS COMPOSITIONS ON THE COMBUSTION CHARACTERISTICS AND EMISSION OF A MODEL COMBUSTOR

Y. S. Sanusi[1,] * and H. A. Dandajeh[2]
[1, 2,] DEPARTMENT OF MECHANICAL ENGINEERING, AHMADU BELLO UNIVERSITY, ZARIA, KADUNA STATE, NIGERIA
Email addresses: [1] *yssanusi@abu.edu.ng*, [2] *hadandajeh@yahoo.com*

ABSTRACT
There is a growing need to design fuel flexible combustors. This require understanding of the combustion and emission characteristics of the combustors under varying fuel compositions. In the present study, the combustion characteristics and emission of methane and syngas flames were investigated numerically in a swirl stabilized combustor. The numerical model was developed using ANSYS-fluent software and validated using experimental values of temperature, CO_2 and NOx emissions. A two-step chemical mechanism was used to model methane-air combustion. Results of the numerical validation showed similar trend between the experimental and predicted temperature along the combustor axis with about 5 % over prediction of the temperature. Syngas-air combustion was thereafter modeled using a 21 step chemical mechanism. Syngas compositions studied were: syngas A (67% CO: 33% H_2), syngas B (50% CO: 50% H_2) and syngas C (33% CO: 67% H_2). Results showed that for pure methane, a V-shaped flame was observed with the flame attached to the fuel nozzle, while a lifted flame was observed for case of syngas A composition. CO gas with higher ignition temperature and flammability as compared to H_2 gas is the dominant gas in syngas A fuel composition. Jet flames were observed for syngas B and syngas C. Carbon monoxide is a slow burning gas. Therefore syngas with low CO content has a low tendency of emission of CO from the combustor. This suggests that syngas with high CO content such syngas A may require more residence time to completely combust the CO gas. The NOx emission was observed to have the same trend as that of the combustor maximum temperature. Syngas C flame had the highest NOx emission, while, syngas A flame had no NOx emission. This is due to low combustor temperature observed in the case of syngas A flame.

Keywords: *Syngas, ANSYS-FLUENT, Swirl-stabilized combustor, NOx emission, Chemical Mechanism*

1. INTRODUCTION

Syngas is a potential energy source for the future due to its wide availability as a product of biofuel and fossil fuel gasification [1], as well as a product of methane reforming. Syngas produced from steam methane reforming (SMR) consist of varying proportion of carbon monoxide (CO) and hydrogen (H_2), and may also contain methane (CH4) depending on its conversion efficiency. The steam required for this process can be generated from solar energy, thereby converting solar thermal energy into chemical energy of the fuel. The continuous variations in solar radiation through the day and across the year as well as the absence of solar radiation at night can have strong effects on the syngas conversion efficiency, and the resultant fuel thermal energy. This affects the heat release rate, emission characteristics and stability of the flame making pilot study necessary. Syngas has been successfully used and proven to be beneficial in commercial plants [2]. Several studies have been carried out with focus on the emissions from syngas combustion. Gadde *et al.* [2] carried out extensive testing on SGT6-5000F combustion system over a range of syngas fuels and achieved NOx and CO

* Corresponding author, tel: +234 – 903 – 257 – 3759

emissions of less than 15 PPM and 10 PPM, respectively. Sainchez *et al*. [3] showed that the use of syngas increases the gas turbine power by 3–7% at generator terminals and 5–10% increase in gas turbine efficiency (LHV based) but resulted in much higher carbon dioxide emissions. Oluyede *et al*. [4] reported that firing syngas in conventional gas turbine can yield over 20-25% power output when compared with the natural gas due to significant flow rate increase. They however, noted that the increase in power output is accompanied by an increase in the moisture content of the combustion products, this is due to higher hydrogen content in the syngas which can contribute significantly to the overheating of the turbine component parts. Performance test of syngas on a GE7EA gas turbine carried out by Lee *et al.* [5] showed that fuel with high hydrogen content emits more NOx, but does not emit CO even in a low load condition while the turbine did not generate combustion pulsation, unlike methane. Khalil *et al.* [6] experimentally studied syngas in a cylindrical combustor with swirling air injection and observed very low-level of NOx (3 PPM) with CO (70 PPM) emissions. Blow off regime is also of interest in syngas study because of its varying composition. This occurs when the characteristic reaction time is longer than the flow residence time in the burner. Fuel compositions and their corresponding flow characteristics are known to have significant effects on the combustor blow off limits. Noble *et al.* [7] experimentally showed that the percentage of H_2 in the fuel dominates the mixture blow off characteristics. Lieuwen *et al.* [1] suggested that the percentage of hydrogen in the fuel is one of the most significant fuel parameter that resists flame blow off due to the hydrogen flame's resistant to stretch induced extinction. Researchers have carried out various works on developing chemical mechanism for syngas modeling [8-16]. Most of the developed mechanisms have been validated against experimental values of laminar flame speeds [17-20]. Other researchers have studied the effects of different fuel compositions [21], nitrogen and carbon dioxide dilutions [22, 23], preheat temperatures and pressures [24, 25] as well as emissions [26-28] on the accuracy of the developed mechanisms. Syngas mechanisms developed have also been used variously in CFD modeling of syngas. In order to provide further insight on the effect of fuel flexibility on gas turbine combustion and emission characteristics. The present study investigated the combustion characteristics and emission in a modeled gas turbine combustor using different syngas compositions and methane gas. The study was carried out numerically using computational fluid dynamics (CFD) approach. CFD combustion study enables researcher to get more insight on the flame dynamics in a cheaper and safer way. It has been used by various researchers [29-31] in the prediction of combustion and emission characteristics.

2. NUMERICAL SCHEME

Syngas combustion characteristics and emission was studied in a vertically positioned swirl-stabilized combustor. The combustor adopted in this study has been used for various experimental studies [32-34]. Air was supplied through an eight-vane swirler with vane angle of 45 degrees and deliver to an orifice of 16mm diameter situated at the combustor dump plane. Fuel was supplied through a nozzle installed on a 6.35-mm-diameter pipe. The fuel nozzle has 16 fuel channels around a centered bluff body of 5mm. The combustion chamber was simulated using a quartz tube that was 70mm in diameter, 300mm long, and 2mm thick. More details of the experimental set-up can be found in [33]. A schematic diagram of the computational geometry of the combustor is given in Figure 1.

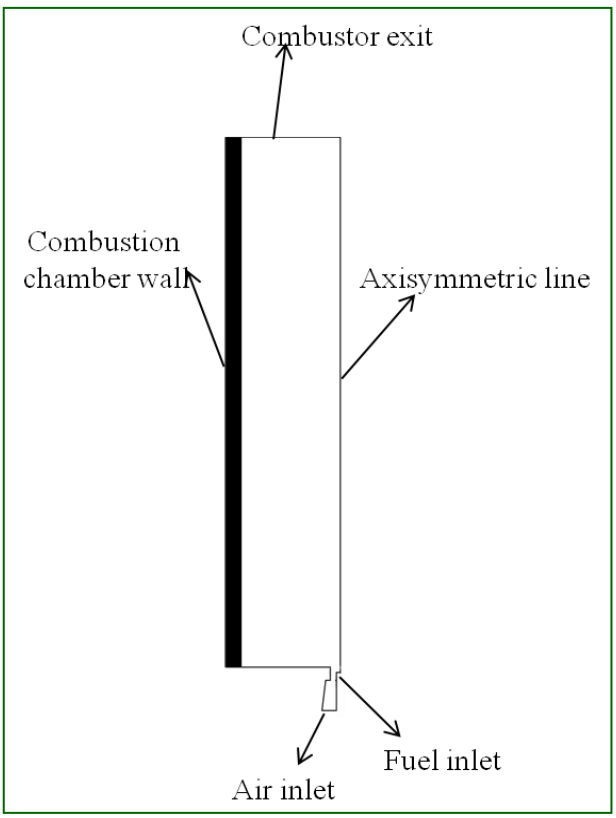

Figure 1. Schematic of the computational domain.

A two-dimensional (2-D) axisymmetric geometry was used to model the combustor due to its (combustor) axial symmetry. More than 70,000 structured, non-uniform grid meshes were used to model the combustor. More cells were used in the high-property gradient regions (i.e., in the vicinity of the wall, inlet, and outlet) to minimize false diffusion errors.

2.1 Governing equations

The generalized equation that governs the conservation of mass, momentum and energy as well as the equation for species transport can be written as [35, 36]:

$$\frac{\partial}{\partial x_j}\left(\rho\bar{u}_j\bar{\emptyset} + \rho\overline{u_j'\emptyset'}\right) = \frac{\partial}{\partial X_j}\left(\Gamma_{\emptyset'}\frac{\partial \emptyset}{\partial x_j}\right) + \bar{\rho}S_{\emptyset} \quad (1)$$

The steady-state mass (eq. 2), momentum (eq. 3), energy (eq. 4) and species (eq. 5) conservation equations for Newtonian fluids were considered:

$$\nabla.(\rho U) = 0 \quad (2)$$

$$\nabla.(\rho UU) = -\nabla P + \mu\nabla^2 U \quad (3)$$

$$(\rho C_p)U.\nabla T = \nabla.(k\nabla T) \quad (4)$$

$$\nabla.(\rho U Y_i) = \nabla.(\rho D_{im}\nabla Y_i) \quad (5)$$

The solution of the continuity (eq. 2) and momentum equations (eq. 3) were solved to obtain the velocity and pressure fields of the gas mixture in the combustor. The energy and species equations were solved to obtain the temperature and species distribution respectively in the combustor. In the present study, the RNG $k-\varepsilon$ model [37, 38] was used for RANS equation closure. The model has an additional term in its ε equation that significantly improves the accuracy for rapidly strained flow. It also accounts for the effect of swirl on turbulence, thus, enhancing the accuracy of swirling flow. A comprehensive details of the model and application can be found in [39].

2.2 Radiation model

The discrete ordinates (DO) radiation model was used to compute the radiative heat exchange between the wall and combustion gases. The weighted sum of gray gases (WSGG) model was used to compute the gas emissivity [37].

2.3 Combustion chemistry

In syngas combustion modelling, Syngas mechanism having 21 elementary steps with 11 species presented in Table 2 was used. The mechanism has been previously used by *Habib et. al.* [29] for syngas modeling in a package boiler. For methane combustion modelling, a two-step global chemical mechanism was used. The constants that appear in the Arrhenius equation for the mechanism is shown in Table 1.

2.4 NOx model

NOx emitted from the combustor was modeled through the post-processing of the main combustion calculation. The NOx calculations that are carried out in the current study are thermal and prompt NOx. The thermal NOx is computed using the extended Zeldovich mechanism with the assumption of quasi-steady state for N and H atoms and partial equilibrium for O [40, 41], while prompt NO is modeled using the expressions proposed by *De Soete* [42].

Table 1. Methane-air combustion equation and Arrhenius constants [30]

	Reaction	A	E_a	Order
CH_4	$CH_4 + 1.5\ O_2 => CO + 2H_2O$	2E+15	34500	$[CH_4]^{0.9}[O_2]^{0.5}$
Mechanism	$CO + 0.5\ O_2 = CO_2$	1E+9	12000	$[CO][O_2]^{0.25}[CO_2]$

Note: the temperature exponent b is zero in all cases

Table 2. Syngas-air combustion equation and Arrhenius constants [30]

	Reaction	A [cm, mol, s]	β	E_a [kJ/mol]
R1	$H + O_2 = OH + O$	2E+14	0	16790.86
R2	$O + H_2 = OH + H$	5.06E+4	2.67	6281.64
R3	$H_2 + OH = H_2O + H$	1E+8	1.60	3296.07
R4	$OH + OH = H_2O + O$	1.5E+9	1.14	100.31
R5	$H + H =M = H_2 + M$ CO/0.75/O_2/0.4/CO_2/1.5/ H_2O/6.5/N_2/0.4	1.8E+18	-1	0
R6	$H + OH + M = H_2O + M$ CO/0.75/O_2/0.4/CO_2/1.5/	2.2E+22	-2	0

	Reaction	A [cm, mol, s]	β	E_a [kJ/mol]
	H_2O/6.5/N_2/0.4			
	O + O + M = O_2 + M			
R7	CO/0.725/O_2/0.4/CO_2/1.5/	2.9E+17	-1	0
	H_2O/6.5/N_2/0.4			
	H + O_2 + M = HO_2 + M			
R8	CO/0.75/O_2/0.4/CO_2/1.5/	2.3E+18	-0.8	0
	H_2O/6.5/N_2/0.4			
R9	HO_2 + H = OH + OH	1.5E+14	0	1003.152
R10	HO_2 + H = H_2 + O_2	2.5E+13	0	692.65
R11	HO_2 + H = H_2O + O	3E+13	0	1719.69
R12	HO_2 + O = OH + O_2	1.8E+13	0	-406.038
R13	OH + HO_2 = H_2O + O_2	6E+13	0	0
R14	HO_2 + HO_2 = H_2O_2 + O	2.5E+11	0	-1241.998
	OH + OH + M = H_2O_2 + M			
R15	CO/0.75/O_2/0.4/CO_2/1.5/	3.23E+22	-2	0
	H_2O/6.5/N_2/0.4			
R16	H_2O_2 + H = H_2 + HO_2	1.7E+12	0	3749.88
R17	H_2O_2 + H = H_2O + OH	1E+13	0	3582.688
R18	H_2O_2 + O = OH + HO_2	2.8E+13	0	6401.07
R19	H_2O_2 + OH = H_2O + HO_2	5.4E+12	0	1003.152
R20	CO + OH = CO_2 + H	6E+6	1.5	-740.42
	CO + O + M = CO_2 + M			
R21	CO/0.75/O_2/0.4/CO_2/1.5/	7.1E+13	0	-4538.07
	H_2O/6.5/N_2/0.4			

3. VALIDATION

In order to validate the governing equations used in this study, experiments were conducted in a swirl stabilized combustor for methane air combustion. Details of the experimental set can be found in [32]. Experiments were carried out with 100% methane and 3.67 MW/m^3 fuel energy input. Temperature profiling along the combustor center line as well as emission from the combustor were recorded. Temperature profiling along the combustor axis was carried out using type R-thermocouple from Omega instruments with measuring range of 1723K and accuracy of 0.25%. Gas chromatography (GC) was used to measure the species concentration at 50 mm from the exit plane of the combustor. The GC used for the species measurement is from Bruker Corporation with model no 450-GC. In measuring the NOx emission, UEI AGA5000 exhaust gas analyzer that has 1 PPM resolution and accuracy of $\pm 5\%$ was used. A still picture was taken to characterize the flame shape (see Figure 2a). A deep blue flame that formed a compact V- shape was observed. The temperature contour was numerically used to depict the flame shape as shown in Figure 2b. The highest flame temperature occurred in the heat release region and, thus, in the vicinity of the flame zone. The predicted combustor temperature also formed a V-shape indicating that the set of equations solved was able to predict the flame shape. In order to have more insight into the flame dynamics and stability, the axial velocity within the combustor was plotted and super-imposed on the contour of heat of reaction contour as shown in Figure 2c. We observed two recirculation zones: the outer recirculation zone (ORZ) and the inner recirculation zone (IRZ).The ORZ is generally formed by the sudden expansion at the dump plane of the combustor while the IRZ is formed by the vortex break down of the flow. The WRZ is formed around the bluff body inserted into the fuel pipe. The contour of the heat of reactions shows that the flames are anchored at the inner shear layer of the flow (between the jet flow and the IRZ) and terminate at the onset of the IRZ. The disappearance of the active reaction zone is due to the vortex rolling up the flame. The vortex roll-up results in the recirculation of a high-temperature combustion product that preheats the incoming fresh charge to the combustor, thus stabilizing the flame. This over prediction in combustion temperature also led to over prediction in the emission as shown in figure 4. The temperature over prediction can be attributed to the

2-step chemical mechanism used in figure 3. This showed a similar trend between the experimental and predicted temperature along the combustor axis was observed. There is about 5 % over prediction of the temperature along the combustor axis. It can however be concluded that the set of governing equations used in this study are adequate for combustion modelling.

4. RESULTS AND DISCUSSION

In the present study, the effects of replacing methane by syngas as fuel on the combustion and emissions characteristics in a model gas turbine combustor were investigated numerically using ANSYS-fluent software. For the purpose of this work, the syngas comprised of only CO and H_2 gas.

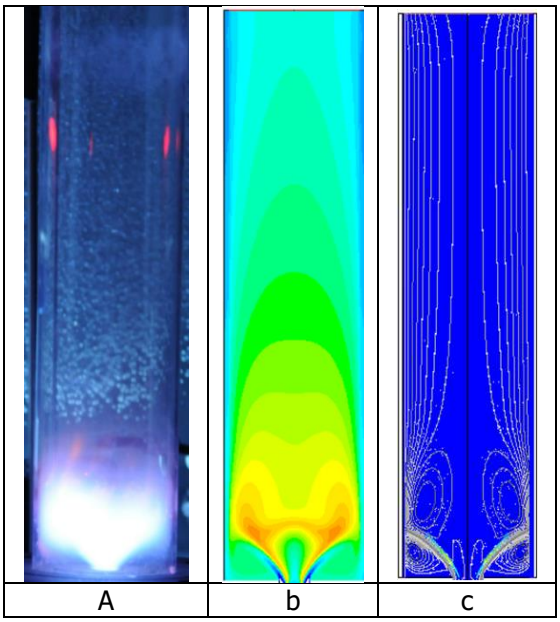

Figure 2. Comparison of the (a) experimental flame picture and numerical (b) temperature contour and (c) flow field.

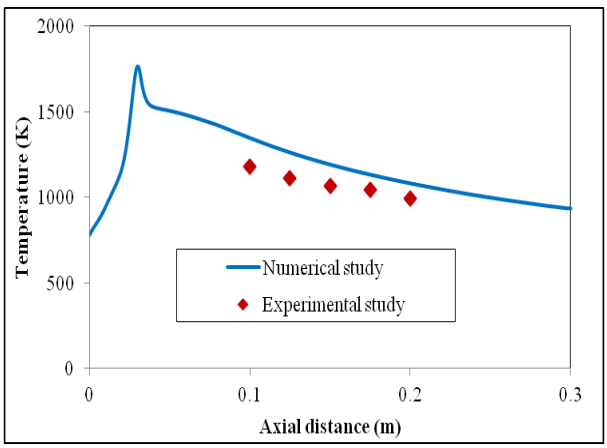

Figure 3. Experimental and numerical temperature along the combustor axis

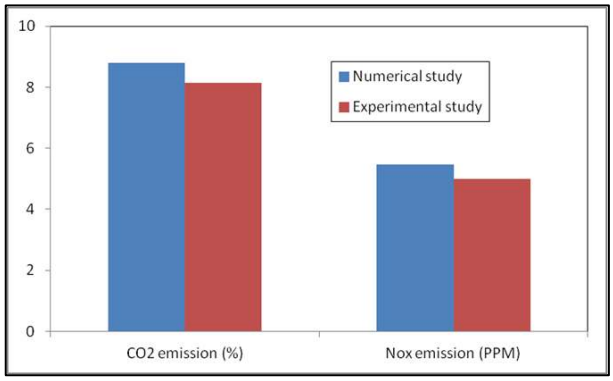

Figure 4. Experimental and numerical pollutant emission at the combustor exit

Due to composition variation that characterizes syngas production, different syngas compositions were studied and categorized as syngas A (67% CO: 33% H_2), syngas B (50% CO: 50% H_2) and syngas C (33% CO: 67% H_2). The combustor firing rate of 3.67 MW/m^3 was maintained for all cases.

The temperature contour has been shown in section 3 to be adequate in characterizing the flame shape. Figure 5 shows the temperature contour over-laid with the axial velocity distribution within the combustor. For pure methane, a V-shaped flame was observed as shown in figure 5 with the flame attached to the fuel nozzle. The flame dynamics is however different from syngas flame. For instance with the case of syngas A, the flame was observed to be stabilized at some distance from the fuel nozzle (i.e. lifted flame). The flow analysis showed that the flame is characterized by three (3) outer recirculation zones (ORZs) with a strong primary and tertiary ORZs and weak secondary ORZ. The flame stabilized in the tertiary ORZ that enable the continuous ignition of the flame. When the hydrogen content in the syngas is increased to 50% (syngas B), the flame became attached to the nozzle. This is because H_2 gas has low ignition temperature (of 500^{o}C) and low flammability limit (4%) as compared to CO gas (609^{o}C and 12 %). The flow analysis shows that ORZs collapsed to a twin ORZ with a jet flame formation. Further increase in the hydrogen content in the syngas (syngas C) lead to a compact ORZ with elongated flame formation. This is due to higher diffusivity of H_2 gas as compare to CO. The graph of the axial velocity along the combustor Centre line shown in figure 6 shows that the presence of inner recirculation zone (IRZ) for methane flame is indicated by negative axial velocity. The IRZ enabled the burnt gas to preheat the fuel/air mixture that lead to rapid fuel consumption of the fuel as shown in Figure 7.

About 99% of methane fuel was consumed at approximately 2.5 cm from the combustor dump plane. Syngas A flame has the highest axial velocity due to its larger ORZ. The domination of syngas A with CO that is slow burning leads the fuel completely burn at about 12 cm from the combustor dump plane. The slow burning rate of syngas A is also visible in the slow temperature rise in the combustor as shown in figure 8. Syngas C flame has the highest combustor temperature. This is because H_2 has the highest adiabatic temperature of 2210°C as compared to CO of 2121°C and methane gas of 1950°C. Therefore burning of syngas fuel with H_2 content of 50% or more require careful design and material selection for the combustor due to high combustion temperature so as to minimize the tendency of material failure. In figure 9, it was shown that decreasing the CO content in the syngas reduce the tendency of emission of CO from the combustor. This is because of the slow burning of CO gas. Therefore, syngas combustor with high CO content must be design to have high residence time to enable the complete burn out of the CO gas. NOx emission was predicted using post combustion processes. The NOx was calculated using the extended Zeldovich mechanism [15] and shown in Figure 11

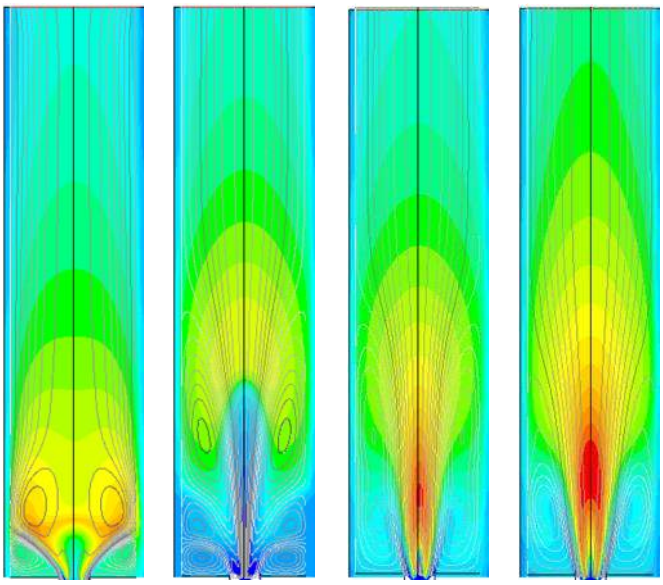

100 % CH_4 | 25% H_2 / 75%CO | 50% H_2 / 50% CO | 75% H_2/ 25% CO

Figure 5. Temperature contour of the combustor temperature over-laid with the flow field for different syngas compositions.

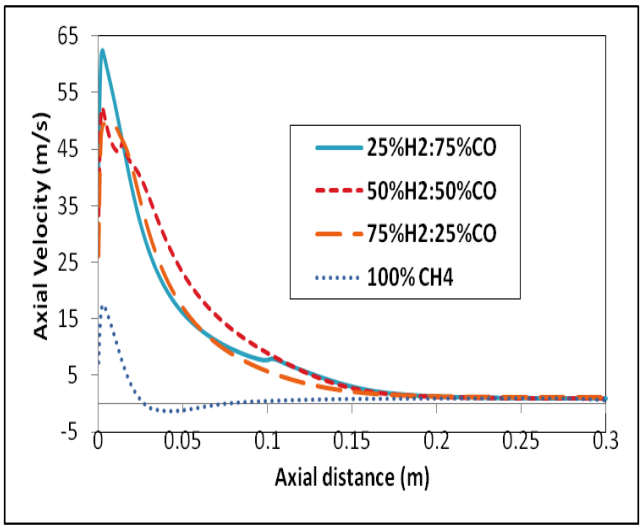

Figure 6. Axial velocity profile along the combustor axis for different syngas compositions.

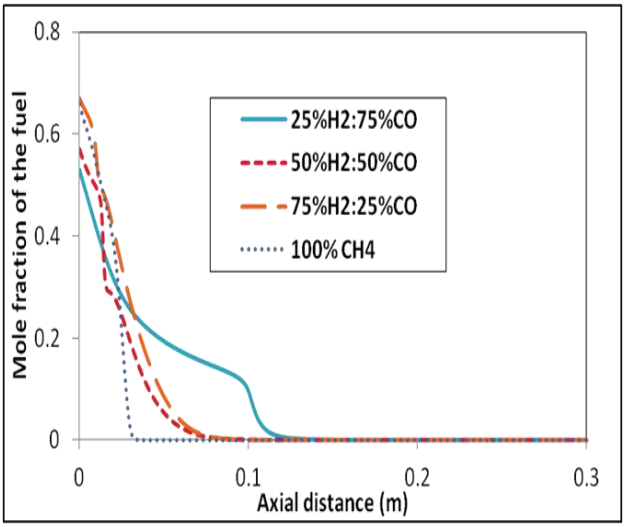

Figure 7. Fuel mole fraction along the combustor axis for different syngas compositions.

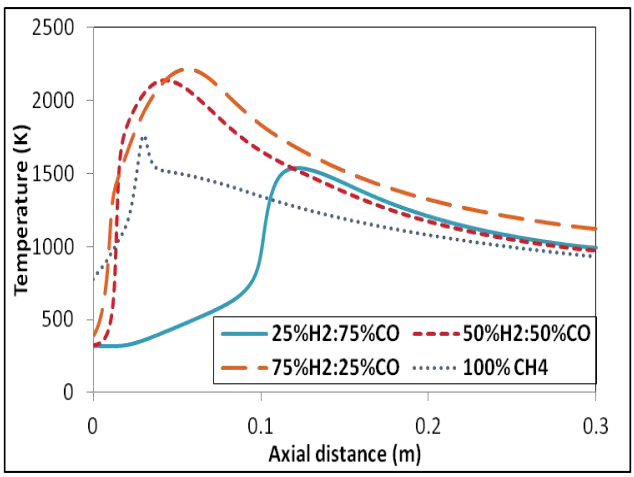

Figure 8. Temperature profile along the combustor axis for different syngas compositions.

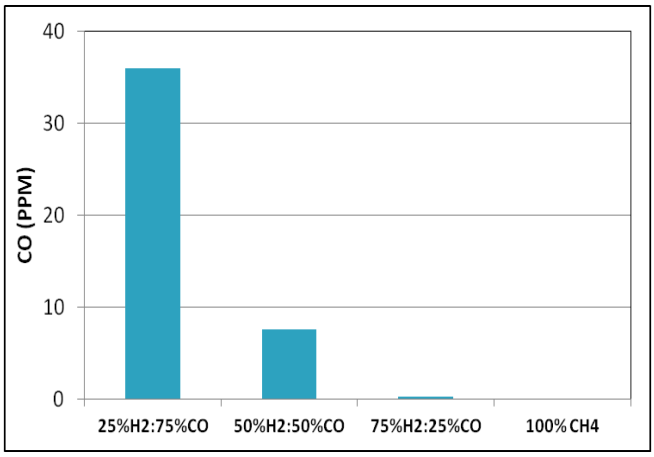

Figure 9. CO emissions for different syngas compositions.

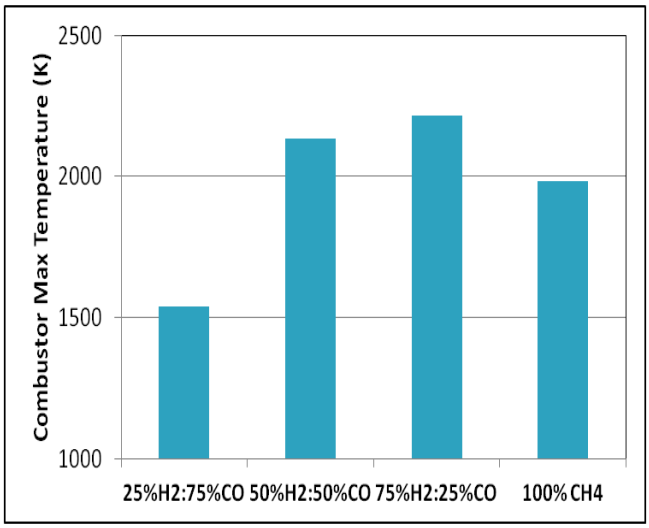

Figure 10. Combustor maximum temperature for different syngas compositions.

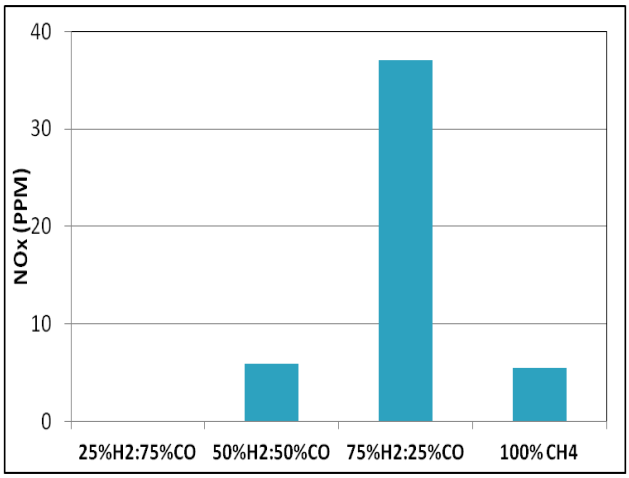

Figure 11. NOx emissions for different syngas compositions.

The NOx emission was observed to have the same trend as that of the combustor maximum temperature as shown in figures 10 and 11. Therefore, any strategy that will lower the maximum temperature such as reducing the equivalence ratio will also lead to the reduction NOx emission. There is no NOx emission for syngas A flame. This due to the fact that no significant amount of NOx are formed at flame temperature of up to 1700 K.

5. CONCLUSION

The present study investigated the combustion characteristics and emission in a model gas turbine combustor for different syngas compositions and methane gas. The study was carried out numerically using computational fluid dynamics (CFD) approach. The following conclusions were drawn:

1. A V-shaped flame was observed with the flame attached to the fuel nozzle for a methane flame, a lifted flame was observed for case of syngas A composition while jet flames were observed for syngas B and syngas C fuel composition.
2. Methane flame is stabilized by inner recirculation zone (IRZ) and outer recirculation zone (ORZ) while syngas flames are stabilized only by the outer recirculation zones (ORZ). Syngas has lower energy density than methane fuel, therefore higher syngas fuel velocity is required to give equivalent (methane) thermal energy in the combustor.
3. The size of the ORZ decreases with increasing hydrogen content in the syngas.
4. The presence of the IRZ in methane flame preheat the fresh charge (methane-air) and leads to rapid consumption of methane fuel.
5. There is no CO emission in methane flame. The CO emission however increases with increasing CO contents in the syngas. Therefore syngas combustor with high CO content must be design to have sufficient residence time to enable the complete burn out of the CO gas.
6. Syngas C flame has the highest NOx emission of about 37 PPM as compared to zero NOx emission observed in syngas A flame. This can be attributed to higher combustor temperature observed in syngas C as compared to other fuel considered.

NOMENCLATURE

B	Temperature exponent	NOx	Nitrogen oxide
CO	Carbon monoxide	P	Pressure magnitude (N/m^2)
CO_2	Carbon dioxide	R_j	species equation source term (kg/m^{3}s)
C_p	specific heat at constant pressure (J/kgK)	$S_\emptyset$	energy source term (W/m^3)
$D_{j,m}$	diffusion flux of specie j (m^2/s)	T	Temperature (K)
E_a	Activation energy (kJ/kmolK)	T_a	ambient temperature (T)
H_2	Hydrogen gas	x	Distance (m)
K_r	Rate constant (m^3/s)	Y_j	Mass fraction of specie j
k_q	Thermal conductivity (W/mK)	ρ	Density (kg/m^3)
M	Unit of length	μ	dynamic viscosity (Ns/m^2)

6. REFERENCES

[1] Lieuwen T, McDonell V, Santavicca D, Sattelmayer T. Burner development and operability issues associated with steady flowing syngas fired combustors. *Combustion Science and Technology*. 2008;180:1169-92.

[2] Gadde S, Wu J, Gulati A, McQuiggan G, Koestlin B, Prade B. Syngas capable combustion systems development for advanced gas turbines. *ASME Paper* GT20006-90970. 2006.

[3] SÃnchez D, Chacartegui R, MuÃoz JM, MuÃoz A, SÃinchez T. Performance analysis of a heavy duty combined cycle power plant burning various syngas fuels. *International Journal of Hydrogen Energy*. 2010;35:337-45.

[4] Oluyede EO, Phillips JN. Fundamental impact of firing syngas in gas turbines. *Proceedings of ASME Turbo Expo 2007* (GT2007). 2007:14-7.

[5] Lee MC, Seo SB, Chung JH, Kim SM, Joo YJ, Ahn DH. Gas turbine combustion performance test of hydrogen and carbon monoxide synthetic gas. *Fuel*. 2010;89:1485-91.

[6] Khalil AEE, Gupta AK. Distributed swirl combustion for gas turbine application. *Applied Energy*. 2011;88:4898-907.

[7] Noble DR, Zhang Q, Shareef A, Tootle J, Meyers A, Lieuwen T. Syngas mixture composition effects upon flashback and blowout. 2006. p. 8-11.

[8] Gregory P. Smith DMG, Michael Frenklach, Nigel W. Moriarty, Boris Eiteneer, Mikhail Goldenberg, C. Thomas Bowman, Ronald K. Hanson, Soonho Song, William C. Gardiner, Jr., Vitali V. Lissianski, and Zhiwei Qin. *GRI-Mech* 3.0 2013.

[9] Davis SG, Joshi AV, Wang H, Egolfopoulos F. An optimized kinetic model of H2/CO combustion. *Proceedings of the Combustion Institute*. 2005;30:1283-92.

[10] Li J, Zhao Z, Kazakov A, Chaos M, Dryer FL, Scire JJ. A comprehensive kinetic mechanism for CO, CH2O, and CH3OH combustion. *International Journal of Chemical Kinetics*. 2007;39:109-36.

[11] Nikolaou ZM, Chen J-Y, Swaminathan N. A 5-step reduced mechanism for combustion of CO/H2/H2O/CH4/CO2 mixtures with low hydrogen/methane and high H2O content. *Combustion and Flame*. 2012.

[12] Marzouk OA, Huckaby ED. A comparative study of eight finite-rate chemistry kinetics for CO/H2 combustion. *Engineering applications of computational fluid mechanics*. 2010;4:331-56.

[13] Frassoldati A, Faravelli T, Ranzi E. The ignition, combustion and flame structure of carbon monoxide/hydrogen mixtures. Note 1: Detailed kinetic modeling of syngas combustion also in presence of nitrogen compounds. *International Journal of Hydrogen Energy*. 2007, 32:3471-85.

[14] Boivin P, Jimenez C, Sanchez AL, Williams FA. A four-step reduced mechanism for syngas combustion. *Combustion and Flame*. 2011;158:1059-63.

[15] Slavinskaya N, Braun-Unkhoff M, Frank P. Reduced reaction mechanisms for methane and syngas combustion in gas turbines. *Journal of engineering for gas turbines and power*. 2008;130.

[16] Cuoci A, Frassoldati A, Faravelli T, Ranzi E. Accuracy and Flexibility of Simplified Kinetic Models for CFD Applications. *Combustion Colloquia-32 nd Combustion meeting*, II-62009. p. 26-8.

[17] Natarajan J, Nandula S, Lieuwen T, Seitzman J. Laminar flame speeds of synthetic gas fuel mixtures. *ASME Paper.* GT2005-68917. 2005.

[18] Dong C, Zhou Q, Zhao Q, Zhang Y, Xu T, Hui S. Experimental study on the laminar flame speed of hydrogen/carbon monoxide/air mixtures. *Fuel.* 2009;88:1858-63.

[19] Bouvet N, Lee SY, Gokalp I, Santoro RJ. Flame speed characteristics of syngas (H2-CO) with straight burners for laminar premixed flames. 2007.

[20] Sun H, Yang SI, Jomaas G, Law CK. High-pressure laminar flame speeds and kinetic modeling of carbon monoxide/hydrogen combustion. Proceedings of the *Combustion Institute*. 2007;31:439-46.

[21] Fu J, Tang C, Jin W, Thi LD, Huang Z, Zhang Y. Study on laminar flame speed and flame structure of syngas with varied compositions using OH-PLIF and spectrograph. *International Journal of Hydrogen Energy*. 2013;38:1636-43.

[22] Prathap C, Ray A, Ravi MR. Effects of dilution with carbon dioxide on the laminar burning velocity and flame stability of H2/CO mixtures at atmospheric condition. *Combustion and Flame*. 2012;159:482-92.

[23] Natarajan J, Lieuwen T, Seitzman J. Laminar flame speeds of H2/CO mixtures: Effect of CO2 dilution, preheat temperature, and pressure. *Combustion and Flame*. 2007;151:104-19.

[24] Yousefian S, Ghafourian A, Darbandi M. NUMERICAL STUDY OF SYNGAS PREMIXED FLAME STRUCTURE AND EXTINCTION. *Chia Laguna*, Cagliari, Sardinia, Italy, September 11-15. 2011.

[25] Monteiro E, Rouboa A. Measurements of the Laminar Burning Velocities for Typical Syngas-Air Mixtures at Elevated Pressures. *Journal of Energy Resources Technology*. 2011;133:031002.

[26] Chun KW, Chung H-J, Chung SH, Choi JH. A numerical study on extinction and NOx formation in nonpremixed flames with syngas fuel. *Journal of mechanical science and technology*.25:2943-9.

[27] Giles DE, Som S, Aggarwal SK. NOx emission characteristics of counterflow syngas diffusion flames with airstream dilution. *Fuel*. 2006;85:1729-42.

[28] Rortveit GJ, Hustad JE, Li S-C, Williams FA. Effects of diluents on NOx formation in hydrogen counterflow flames. *Combustion and Flame*. 2002;130:48-61.

[29] Habib MA, Mokheimer EM, Sanusi SY, Nemitallah MA. Numerical investigations of combustion and emissions of syngas as compared to methane in a 200 MW package boiler. *Energy Conversion and Management*. 2014;83:296-305.

[30] Mokheimer E, Sanusi YS, Habib MA. Numerical study of hydrogen-enriched methane–air combustion under ultra-lean conditions. *International Journal of Energy Research*. 2015.

[31] Sanusi YS, Mokheimer EM. Performance analysis of a membrane-based reformer-combustor reactor for hydrogen generation. *International Journal of Energy Research*. 2018.

[32] Sanusi YS, Habib MA, Mokheimer EM. Experimental study on the effect of hydrogen enrichment of methane on the stability and emission of nonpremixed swirl stabilized combustor. *Journal of Energy Resources Technology*. 2015;137:032203.

[33] Sanusi YS, Mokheimer EM, Shakeel MR, Abubakar Z, Habib MA. Oxy-Combustion of Hydrogen-Enriched Methane: *Experimental Measurements and Analysis. Energy & Fuels*. 2017;31:2007-16.

[34] Abubakar Z, Sanusi S, Mokheimer EM. Experimental Analysis of the Stability and Combustion Characteristics of Propane–Oxyfuel and Propane–Air Flames in a Non-premixed, Swirl-Stabilized Combustor. *Energy & Fuels*. 2018;32:8837-44.

[35] Reynolds WC. Fundamentals of turbulence for turbulence modeling and simulation. *Lecture Notes for Von Karman Institute*, Agard Report No 755. 1987.

[36] Shih T-H, Liou WW, Shabbir A, Yang Z, Zhu J. A new k-*e* eddy viscosity model for high reynolds number turbulent flows. *Computers & Fluids*. 1995;24:227-38.

[37] Yakhot V, Orszag SA. Renormalization group analysis of turbulence. I. Basic theory. *Journal of scientific computing*. 1986;1:3-51.

[38] Smith LM, Woodruff SL. Renormalization-group analysis of turbulence. *Annual Review of Fluid Mechanics*. 1998;30:275-310.

[39] Orszag SA, Yakhot V, Flannery WS, Boysan F, Choudhury D, Maruzewski J, et al. Renormalization group modeling and turbulence simulations. *Near-wall turbulent flows*. 1993:1031-46.

[40] Lobert JM, Warnatz J. Emissions from the combustion process in vegetation. Fire in the environment: *The ecological, atmospheric, and climatic importance of vegetation fires*. 1993:15-37.

[41] Gobbato P, Masi M, Toffolo A, Lazzaretto A, Tanzini G. Calculation of the flow field and NO x emissions of a gas turbine combustor by a coarse computational fluid dynamics model. *Energy*. 2012;45:445-55.

[42] De Soete GG. Overall reaction rates of NO and N 2 formation from fuel nitrogen. *Symposium (international) on combustion*: 1975. p. 1093-102.

[43] Ghenai C. Combustion of Syngas Fuel in Gas Turbine Can Combustor. *Advances in Mechanical Engineering*. 2010;2010.

[44] Wan J, Fan A, Maruta K, Yao H, Liu W. Experimental and numerical investigation on combustion characteristics of premixed hydrogen/air flame in a micro-combustor with a bluff body. *International Journal Of Hydrogen Energy*. 2012;37:19190-7.

[45] Nemitallah MA, Habib MA. Experimental and numerical investigations of an atmospheric diffusion oxy-combustion flame in a gas turbine model combustor. *Applied Energy*. 2013;111:401-15.